


Long non-coding RNA LOC554202 modulates chordoma cell proliferation and invasion by recruiting EZH2 and regulating miR-31 expression

Xianli Ma¹ | Shengjin Qi² | Zhenying Duan² | Hongzhan Liao² | Baohua Yang² |
Wenbo Wang² | Jie Tan³ | Qinghua Li³ | Xuewei Xia² 

¹College of Pharmacy, Guilin Medical University, Guilin, Guangxi, China

²Department of Neurosurgery, Affiliated Hospital of Guilin Medical University, Guilin, Guangxi, China

³Guangxi Key Laboratory of Brain and Cognitive Neuroscience, Guilin, Guangxi, China

Correspondence

Xuewei Xia, Department of Neurosurgery, Affiliated Hospital of Guilin Medical University, Guilin, Guangxi, China.
Email: xxw7456@163.com

Funding information

This research was supported in part by The National Natural Science Foundation of China (No. 81560413), The Natural Science Foundation for Returned Scholars of Guangxi (2016GXNSFCA380028) and the Innovative Project of Guangxi Key Laboratory of Brain and Cognitive Neuroscience.

Abstract

Objectives: Chordoma is a rare malignant bone tumour arising from notochordal remnants. Long non-coding RNA LOC554202, as the host gene of miR-31, contributes to various cancer developments. However, little is known about the biological function of LOC554202 in chordoma. Here, the relationship between LncRNA LOC554202, miR-31 and EZH2 was elucidated in chordoma.

Materials and methods: The levels of LOC554402, miR-31, EZH2, RNF144B, and epithelial-mesenchymal transition (EMT) markers were measured in chordoma tissues and the chordoma cell lines via quantitative real-time PCR (qRT-PCR) or Western blot. FISH assay demonstrated the LOC554402 expression in chordoma tissues. The chordoma cell lines, U-CH1 and JHC7, were transfected with siRNA or miRNA mimics and analysed for cell proliferation ability, apoptosis, cell migration, and invasion. RNA pull down, RIP assay, and Luciferase Reporter Assay were used to analyze the interaction between LOC554202 and EZH2. Animal tumour xenografts were generated, and qRT-PCR was performed to investigate EZH2, miR-31, and RNF144B expression on tumour growth in vivo.

Results: We found elevated expression of LOC554202 was associated with a decreased level of miR-31 in cancer tissues. Knockdown of LOC554202 or overexpression of miR-31 suppressed the proliferation, migration, and invasion of chordoma cells. Unexpectedly, EZH2 as a binding protein of LOC554202, and it was positively regulated by LOC554202, leading to the reduced expression of miR-31. Furthermore, the impaired function of miR-31 restored expression of the oncogene RNF144B and maintained the metastasis-promoting activity in vitro. The results in vivo confirmed the anti-tumour effects of knockdown of LOC554202, which inhibited EZH2/miR-31 to activate the oncogene RNF144B.

Conclusion: Our results suggest that LOC554202 may play an important role in the progression of chordoma by the direct upregulation of EZH2 and indirect promotion of RNF144B via miR-31.

1 | INTRODUCTION

Chordoma is a rare bone tumour arising from malignant transformation of cellular remnants of the embryonic notochord,¹ is characterized as highly recurrent, aggressive and locally invasive, and occurs most commonly at the sacrococcygeal and skull base region.^{2,3} The tumour predominantly affects older male adults.⁴ To date, surgical resection is the first choice for the treatment of chordoma, which is highly resistant to chemotherapy and radiotherapy.⁵ However, there is still frequent local recurrence and eventual metastasis after surgical measures for.^{6,7} Therefore, knowledge about the molecular biology process underlying chordoma progression will help us better understand this disease and develop effective targeted therapies.

According to the genome data, the human transcriptome consists largely of non-coding RNAs (ncRNAs), which are defined as endogenous regulatory RNAs and broadly classified into short ncRNAs and long ncRNA (lncRNAs) based on size.^{8,9} lncRNAs (more than 200 nucleotides in length) have recently been shown to play a critical role in biological functions correlated with human diseases, especially cancer.¹⁰⁻¹² MicroRNAs (miRs), which are short non-coding RNA sequences of usually 20-30 nucleotides, also act as tumour suppressors as well as oncogenes regulating post-transcriptional gene expression involved in many cancer types, including chordoma.¹³⁻¹⁵ Interestingly, lncRNA is found to interact with miRs as it competes with endogenous RNA in various pathological mechanisms. For example, lncRNA H19 contributes to glucose metabolism in muscle cells inhibiting miR let-7 expression.¹⁶ lncRNA-p21 can enhance PTEN expression by competitively binding miR-181b in liver fibrosis.¹⁷

lncRNA loc554202 (LOC554202) is a non-protein-coding gene located on human chromosome 9p21.3 and was recently reported to be downregulated in colorectal cancer,¹⁸ but overexpressed breast cancer cells,¹⁹ suggesting that LOC554202 might function as anti-oncogene or oncogene similar to protein-coding genes in these types of cancers. Studies have shown that LOC554202 is the host gene of miR-31 and regulates its transcriptional level,^{19,20} as further verified in triple-negative breast cancer.²¹ Most recently, Bayrak et al found that miR-31 was significantly downregulated in chordomas and that its overexpression suppressed chordoma cancer cell proliferation by inducing apoptosis,²² which indicated that miR-31 might be closely correlated with chordoma progression. These results further prompted us to investigate the biological functions of LOC554202 and the relationship between LOC554202 and miR-31 in chordoma.

In the present study, we examined the expression of LOC554202 and miR-31 in chordoma tissues and performed loss-of-function and gain-of-function experiments in chordoma cell lines and evaluated proliferation, migration, invasion, and apoptosis. We also elucidated the molecular mechanisms underlying the relationship between LOC554202 and miR-31, which will aid us to find potential therapeutic targets in the treatment of patients with chordoma.

2 | MATERIALS AND METHODS

2.1 | Chordoma tissues samples

A total of 20 pairs of fresh chordoma and normal tissue specimens were obtained from patients who had undergone surgical resection of chordoma in the Affiliated Hospital of Guilin Medical University. None of the enrolled patients had received any chemotherapy or radiotherapy before surgical excision of the tumour lesion. Before participation in this study, each patient signed written informed consent forms. This study was approved by the hospital ethics committee of the Affiliated Hospital of Guilin Medical University.

2.2 | Cell lines and transfection

The chordoma cell lines, U-CH1 and JHC7, were obtained from the American Type Culture Collection (Manassas, VA). U-CH1 cells were cultured in IMDM-RPMI media (4:1) supplemented with 10% FBS and 1% penicillin-streptomycin. JHC7 cells were grown in DMEM media containing 10% FBS and 1% penicillin-streptomycin. These two cell lines were maintained in a humidified 5% CO₂-enriched atmosphere at 37°C.

To construct the LOC554202 and RNF144B knockdown cell models, U-CH1 and JHC7 cells were transfected with siRNAs against LOC554202 and RNF144B to generate U-CH1/siLOC554202, U-CH1/siRNF144B, JHC7/siLOC554202, and JHC7/siRNF144B, respectively. For overexpression of miR-31, U-CH1 and JHC7 cells were transfected with miR-31 mimics, with negative control (NC) as control. All transfections were carried out using Lipofectamine 2000 (Invitrogen, Carlsbad, CA) according to the manufacturer's instruction. All of the siRNAs and miR-31 mimics used in the study were synthesized by GenePharma Company (Shanghai, China).

2.3 | Quantitative real-time PCR (qRT-PCR) analysis

Total RNA was extracted from tissues and cells using TRIZOL reagent (Invitrogen, Carlsbad, CA, Life Technologies, Carlsbad, CA) according to the manufacturer's protocols. For qRT-PCR, 1 µg of total RNA was reverse transcribed to cDNA using Reverse Transcription Kit (Takara, Dalian, China). Gene expression was determined using Fast Real-time PCR 7500 System (Applied Biosystems, Foster City, CA). The PCR reaction was set for 50°C for 2 minutes, followed by 40 cycles of 95°C for 15 seconds, then 60°C for 1 minute. GAPDH was amplified as the internal control for LOC554202 and mRNAs. U6 snRNA was used to normalize the relative abundance of miR-31. The expression levels (2- $\Delta\Delta$ Ct) of LOC554202, mRNAs, and miR-31 were calculated as described previously.²³ The primer pair that was used is shown in Table 1.

2.4 | Fluorescence in situ hybridization (FISH)

Probes for MIR31HG-FISH were purchased from Ribobio Company (Guangzhou, China), U6 and 18S were used as cytoplasmic and nuclear positive control. Frozen sections of tumour tissues were

TABLE 1 Primers used in qPCR assays

Gene	Primer 5'-3'
Cytokeriatin	F: GAAATCAGTACGCTGAGGGG R: CCGGCTGGTGAACCAGGCTT
E-cadherin	F: TCCATTCTTGGTCTACGCC R: CACCTTCAGCCATCCTGTTT
Vimentin	F: GGCTCGTCACCTTCGTGAAT R: TCAATGTCAAGGGCCATCTTAA
N-cadherin	F: GTGCCATTAGCCAAGGGAATTCAGC R: GCGTTCCTGTTCCACTCATAGGAGG
GAPDH	F: ACCCACTCCTCCACCTTTGA R: CTGTTGCTGTAGCCAAATTCGT

briefly thawed, permeabilised with 0.5% TX in PBS for 8 minutes on ice, fixed in 4% formaldehyde/5% acetic acid/0.14 M NaCl for 18 minutes at room temperature, washed in PBS, dehydrated in 70%-100% ethanol series and air-dried for the hybridization with MIR31HG probes according to the the manufacturer's protocols. The coverslips were mounted onto the glass slides with neutral gum and observed by FV10i confocal microscope (OLYMPUS, Japan).

2.5 | EdU flow cytometry assay

To measure cell proliferation rates, EdU incorporation experiments were performed using the Cell Light™ EdU Apollo®488 In Vitro Imaging Kit (Ribobio, Guangzhou, China) according to the manufacturer's protocol. Briefly, cells were transfected with miR-31 mimic, siLOC554202, siRNF144B or NC for 48 hour and then incubated with 50 μM of EdU labelling medium for 2 hour at 37°C. Then cells were fixed with 4% paraformaldehyde (50 μL per well) for 20 minutes and incubated with glycine (2 mg/mL). About 5 minutes later, the cells were washed with PBS three times and stained with 200 μL 1× Apollo solution for 30 minutes at 37°C in dark. After washing with 0.5% TritonX-100 in PBS for 5 minutes, the percentage of EDU positive cells was detected by flow cytometry with the Cytomics FC 500 MCL (Beckman Coulter, Brea, CA). Each experiment was performed in triplicate and repeated three times.

2.6 | Colony formation assay

To evaluate monolayer colony formation, stably transfected U-CH1 and JHC7 cells from different groups (control, NC, miR-31, or siLOC554202) were plated into six-well plates at a density of 600 cells per well and incubated for 7 days. Then cells were fixed with paraformaldehyde and stained with 1% crystal violet (Beyotime) as previously reported.²⁴ The colonies that were formed (more than 50 cells per colony) were observed using Image-Pro Plus 6.0 software (Media Cybernetics, MD) and manually counted under light microscopy. Each experiment was performed in triplicate and repeated three times.

2.7 | Hoechst staining assay

Cells were cultured in six-well plates for 48 hours after transfection and incubated with Hoechst 33 342 (5 μg/mL, Sigma, St. Louis, MO) for 10 minute at room temperature. Following washing with 0.5% TritonX-100 in PBS, the changes in nuclear morphology were observed under a fluorescence microscope (OLYMPUS, Tokyo, Japan). Each experiment was performed in triplicate and repeated three times.

2.8 | Cell migration and invasion assay

Cell migration/invasion was observed using Transwell chambers (8.0 mL pore size; Costar, Washington, D.C.) following the manufacturer's instructions. Briefly, cells were suspended in serum-free medium and seeded into upper chambers that were either uncoated (for migration assay) or coated (for invasion assay) with BD Matrigel™ Basement Membrane Matrix. A volume of 0.6 mL of 20% FBS medium was added to the lower Transwell chamber as a chemoattractant. After incubation for 24 hours, cells that migrated to the bottom chamber from the upper chamber were fixed in 4% paraformaldehyde and stained with 0.1% Crystal Violet Staining Solution. The number of cells that migrated to the bottom chamber was counted under a microscope in five random fields, and the average number was calculated. Each experiment was performed in triplicate and repeated three times.

2.9 | Tumour xenograft model and tumour formation assay

Stably transfected U-CH1 and JHC7 cells (4×10^6 cells/mouse, 0.2 mL) were subcutaneously injected into 5-week-old male NOD-SCID nude mice provided from Shanghai Laboratory Animals Center of the Chinese Academy of Sciences (Shanghai, China). Tumour volumes were examined and calculated every 7 days using the following formula: $0.5 \times \text{length} \times \text{width}^2$. This study was approved by the Committee on the Ethics of Animal Experiments of the Affiliated Hospital of Guilin Medical University.

2.10 | RNA pull down assay

The expression vector pcDNA3.0-LOC554202 and pcDNA3.0-GAPDH were first labelled with biotin-UTP via in vitro transcription. Biotin-labelled LOC554202 and GAPDH were incubated with HEK293 cell pellets overexpressing flag-EZH2. Then a total of 20 μL washed High Capacity Streptavidin Agarose Beads (Thermo, Rockford, IL) was added to the above mixture and incubated for 1 hour. After three washes in salt wash buffer, the beads were boiled in SDS buffer. Subsequently, EZH2 protein was detected using anti-Flag by Western blot.

Recombinant GST-EZH2 was purified using GST-agarose affinity chromatography. A total of 5 μg of GST-EZH2 protein was incubated with 2 μg of biotinylated LOC554202 and GAPDH in 200 μL binding buffer for 1 hour. Similarly, 20 μL of washed High Capacity Streptavidin Agarose beads (Thermo) were added to the binding

reaction and incubated for 30 minutes, then washed according to the above method. All binding reactions and washes were carried out in room temperature. Retrieved protein was also determined using Western blot.

2.11 | RNA immunoprecipitation (RIP) assay

RNA immunoprecipitation was used to investigate whether ribonucleoprotein complex contained LOC554202 and its potential binding protein EZH2 in chordoma cells using the Magna RIP RNA-binding protein immunoprecipitation kit (Millipore) according to the manufacturer's instructions. qRT-PCR was performed to detect the co-precipitated RNAs with the total RNAs as the input controls.

2.12 | Luciferase activity assay

The 3'-UTR sequence of RNF144B containing the binding site of miR-31 was cloned into the psiCHECK™-2 vector. 293T cells were cultured in 6-well plates and transfected with 100 ng of psiCHECK-RNF144B-3'-UTR vector containing firefly luciferase together and 50 ng of miR-31 mimics or negative control or mutational miR-31 mimics. Transfection was performed using Lipofectamine 2000 (Invitrogen). At 24 hour post-transfection, Dual-Luciferase Reporter Assay (Promega) was performed to calculate the relative luciferase activity by normalizing the Firefly luminescence to the Renilla luminescence according to the manufacturer's instructions.

2.13 | Western blot assay

Total protein was extracted by lysing cells in RIPA buffer with Protease Inhibitor Cocktail (Pierce). BCA Protein Assay Kit (Beyotime) was used to measure the protein concentration. Equivalent amounts of protein were separated by 10% SDS-PAGE polyacrylamide gels and then transferred to PVDF membranes (Millipore). The membranes were blocked with 5% non-fat milk in Tris-buffered saline and then incubated with primary antibodies followed by horseradish peroxidase-conjugated secondary antibody (Abcam). The protein signals were detected by ECL chemiluminescence kit and quantified using Image J software. GAPDH was used as a loading control. The primary antibodies used were specific for EZH2 (#5246; Cell Signaling Technology, Danvers, MA), RNF144B (#42516; BD Biosciences, Franklin Lakes, NJ), cytokeratin (ab76126; Abcam, Cambridge, UK), E-cadherin (#3195; Cell Signaling Technology), vimentin (ab92547; Abcam), N-cadherin (#13110; Cell Signaling Technology), and GAPDH (#2128; Abcam).

2.14 | Immunohistochemistry

Tissue expression of EZH2 protein was examined using immunohistochemistry. Briefly, tissues were fixed in 10% formaldehyde and cut into 4- μ m-thick slices. They were then deparaffinized in xylene and rehydrated in graded alcohol. The sections were washed and then immunostained

using DAB plus kit (Maixin, Fuzhou, China) after incubating with primary antibody (1:5000, Sigma, St. Louis, MO) at 4°C overnight. Staining under 20% of the tissue or no staining was included in the negative group, while the others belonged to the positive groups.

2.15 | Statistical analysis

All data were shown as mean \pm SD. All statistical analyses were performed using SPSS 17.0 software. Student's *t* test was used to determine the statistical significance between two groups in vitro and in vivo experiments. A two-tailed value of $P < .05$ was considered statistically significant.

3 | RESULTS

3.1 | Expression of LOC554402 and miR-31 in chordoma tissues

qRT-PCR assay was used to determine the expression of LOC554202 and miR-31 in 20 paired clinical chordoma and non-tumour tissues. As shown in Figure 1A, the mRNA levels of LOC554202 were significantly upregulated in chordoma tissues compared with matched non-tumour tissues ($P < .001$). Meantime, to confirm the expression pattern of LOC554302 in patients with chordoma, FISH was performed to determine the presence by LOC554302-target DNA probe. The results indicated that positive staining of LOC554302 in three different patients. In contrast, the expression of miR-31 was observed to be downregulated in tumour tissues compared with paired non-tumour tissues (Figure 1B, $P < .001$). Statistical analysis further demonstrated that the transcription of LOC554202 was inversely correlated with miR-31 expression (Figure 1C, $P = .001$).

3.2 | LOC554202/miR-31 affects cell proliferation and apoptosis in chordoma

To investigate the biological functions of LOC554402 and miR-31 in chordoma, we then selected two chordoma cell lines, U-CH1 and JHC7 to carry out loss-of-function and gain-of-function experiments. As depicted in Figure 2A, 5-ethynyl-2'-deoxyuridine (EdU) flow cytometry revealed that the percentage of EdU positive cells reached 10.0% in miR-31 mimics group and 7.0% in the siLOC554202 group, which were substantially reduced compared with that of control and NC groups in U-CH1 cells. Similar results were also found in JHC7 cells. In addition, the colony formation assay revealed that inhibition of LOC554202 or overexpression of miR-31 substantially impaired cell colony formation ability, as indicated by the formation of fewer and smaller colonies in U-CH1 and JHC7 cells (Figure 2B). These data provide evidence of the growth-promoting role of LOC554202 and the growth-suppressing role of miR-31 in vitro.

To confirm whether cell growth inhibition was caused by apoptosis, we performed Hoechst staining and flow cytometric analysis in

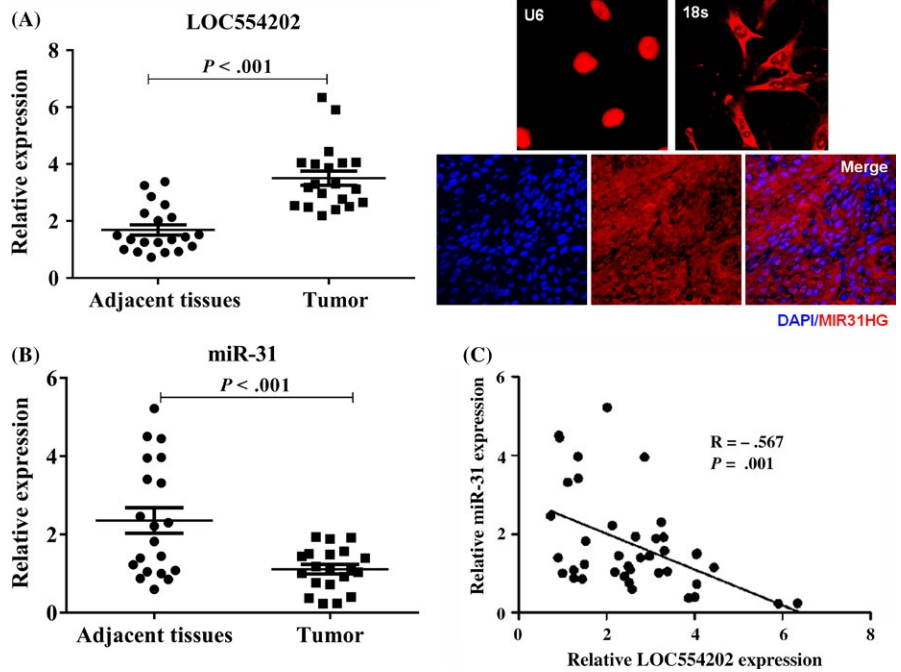


FIGURE 1 Loc554202 and miR-31 were aberrantly expressed in chordoma tissues. Quantitative real-time PCR (qRT-PCR) was performed to measure the mRNA levels of LOC554202, and its expression pattern was determined by FISH (A) and miR-31 (B). The correlation between LOC554202 and miR-31 was also analyzed (C)

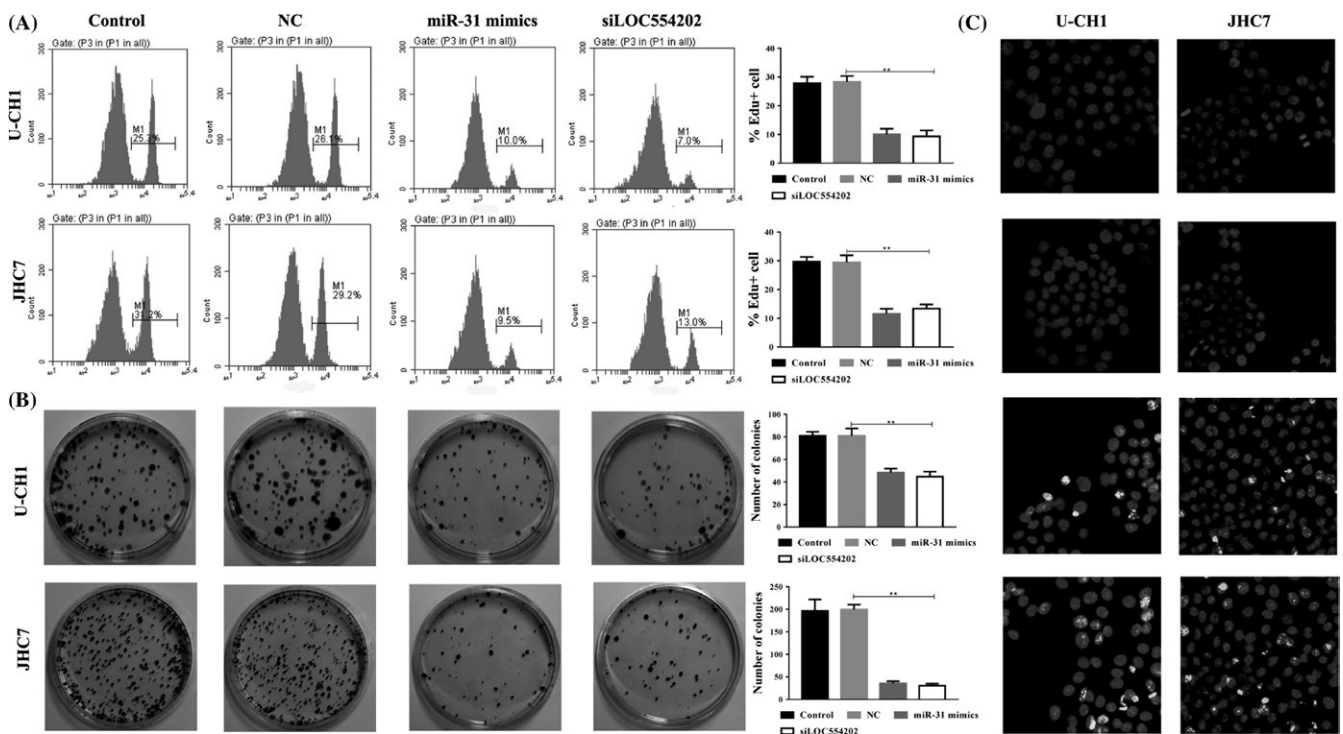


FIGURE 2 The effects of LOC554202 and miR-31 on chordoma cell proliferation and apoptosis in vitro. Chordoma cells were transfected with siLOC554202, miR-31 mimics, or empty vector control. A, EdU flow cytometry was used to analyze the percentage of EdU positive cells in U-CH1 and JHC7 cells after transfection with siLOC554202, miR-31 mimics, NC, or empty vector, respectively. B, A colony formation assay was performed to determine the role of LOC554202 or miR-31 in cell proliferation in U-CH1 and JHC7 cells. C, Hoechst staining assay was performed to determine the number of cells with condensed and fragmented nuclei, indicating cell apoptosis. $**P < .01$

siLOC554202- or miR-31-treated U-CH1 and JHC7 cells. As shown in Figure 2C, notably higher number of cells with condensed and fragmented nuclei (indicating early apoptotic cell fraction) were observed in siLOC554202 or miR-31 mimics-treated U-CH1 and JHC7

cells compared with NC-treated or control U-CH1 and JHC7 cells. Collectively, these results indicated that knockdown of LOC554202 or overexpression of miR-31 could suppress chordoma cell proliferation and induce apoptosis in vitro.

3.3 | LOC554202/miR-31 affects cell migration and invasion in chordoma by altering EMT expression

We further assessed the effects of LOC554202 and miR-31 on cell migration and invasion, which are key determinants of malignant progression and metastasis. Using a Transwell system, we found the migratory and invasive ability of U-CH1 and JHC7 cells was significantly decreased following siLOC554202 or miR-31 mimics transfection (Figure 3A). Then we detected the expression of classical epithelial-mesenchymal transition (EMT) markers, including cytokeratin, E-cadherin, N-cadherin, and vimentin by qRT-PCR and Western blot analysis. As shown in Figure 3B, the mRNA levels of cytokeratin and E-cadherin were dramatically elevated, while mRNA levels of N-cadherin and vimentin were significantly decreased in LOC554202 knockdown or miR-31 overexpressed chordoma cells ($P < .01$, $P < .001$). Consistent with the qRT-PCR results, the protein levels of EMT markers presented similar trends in U-CH1 and JHC7 cells following siLOC554202 or miR-31 mimics transfection (Figure 3C). These results further indicated that LOC554202/miR-31 altered cell migratory and invasive ability by regulating the EMT process of chordoma cells.

3.4 | LOC554202 silenced miR-31 expression by directly recruiting EZH2

Previous research findings have indicated that lncRNAs play an important role in regulating tumour cell growth via binding to enhancer of zeste homolog-2 (EZH2) in many cancers.^{25,26} Thus we analyzed the interaction between LOC554202 and EZH2 by RNA pull down and RIP assay. As shown in Figure 4A, EZH2 was specifically retrieved by purified biotinylated LOC554202 RNA in HEK293 cells transfected with a Flag-EZH2 expressing vector. Furthermore, purified GST-EZH2 was observed to be bound to biotinylated LOC554202 in vitro (Figure 4B). Furthermore, results of RIP assay revealed that LOC554202 RNA was more highly enriched by antibody against EZH2 in chordoma cells compared with the IgG control (Figure 4C). In summary, these results demonstrated a direct interaction between LOC554202 and EZH2. To further confirm these results, the effects of LOC554202 overexpression on EZH2 and miR-31 were analyzed using qRT-PCR, which showed that overexpression of LOC554202 significantly increased the relative mRNA level of EZH2 (Figure 4D), and the tumour tissues also showed higher expression of EZH2 compared with relative normal tissue (Figure 4E). The expression of miR-31 was inhibited by

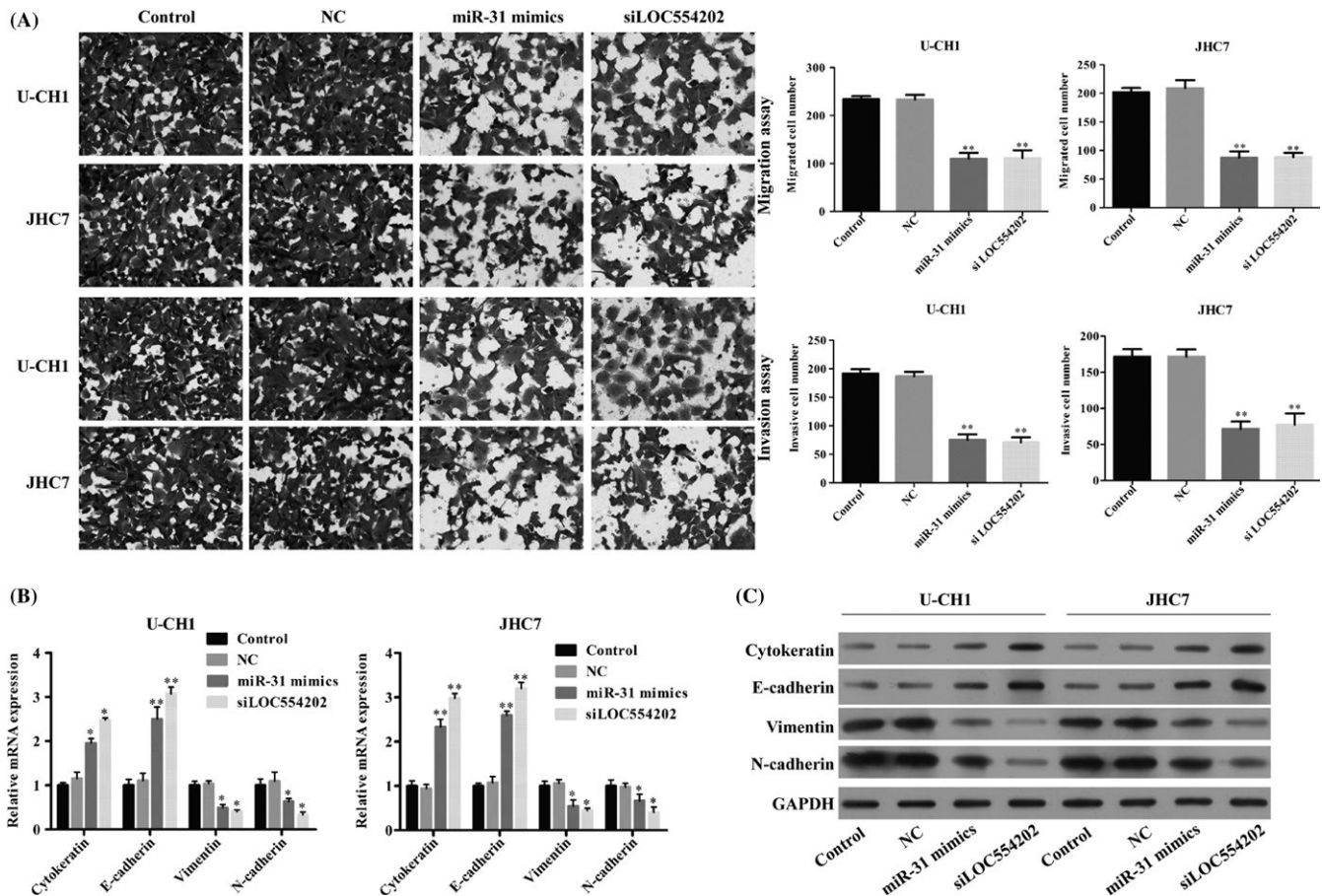


FIGURE 3 The effects of LOC554202 and miR-31 on chordoma cell migration and invasion in vitro. A, Transwell assay was used to determine cell migratory and invasive ability in U-CH1 and JHC7 cells following siLOC554202 or miR-31 mimics transfection. B, The mRNA levels of cytokeratin, E-cadherin, N-cadherin, and vimentin were detected by qRT-PCR. * $P < .05$, ** $P < .01$ vs NC or control, Student's *t* test. C, The protein levels of cytokeratin, E-cadherin, N-cadherin, and vimentin were evaluated by Western blot

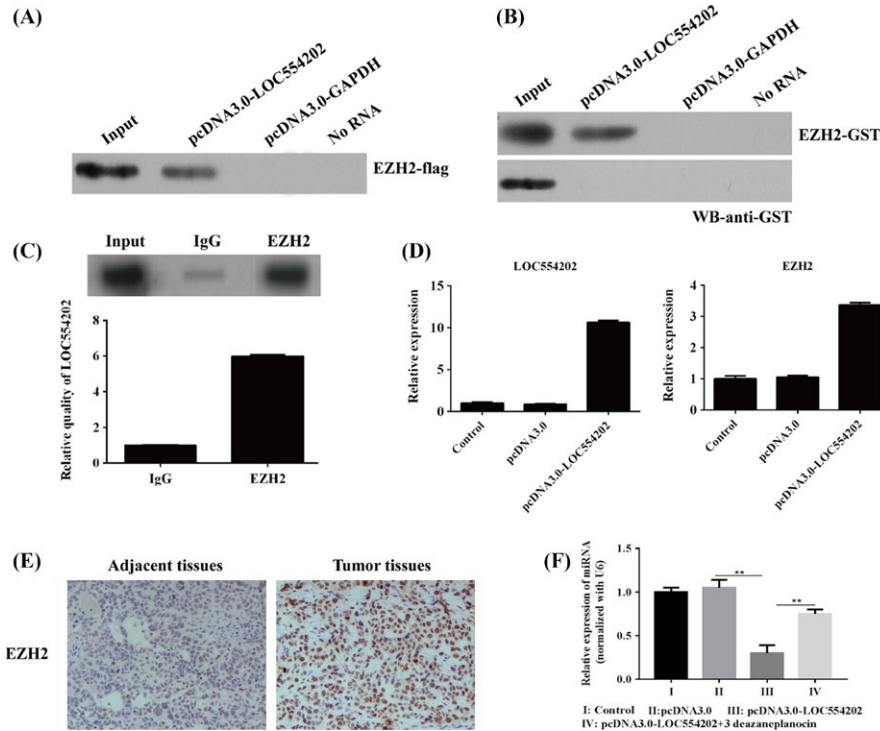


FIGURE 4 LOC554202 silenced miR-31 expression by directly recruiting EZH2. A, Western blot of EZH2 protein bound to in vitro transcribed biotinylated LOC554202 incubated with extracts of 293T cells that were transfected with Flag-EZH2 vector. B, In vitro transcribed biotinylated LOC554202 retrieved purified GST-EZH2 but not GST. C, RIP experiments were performed using an antibody against EZH2 on extracts from chordoma cells. Protein immunoprecipitated from cell extracts by EZH2 antibody or IgG was detected by Western blot analysis. Purified RNA was used for qRT-PCR. D, The expression of LOC554202 and EZH2 were determined in chordoma cells following LOC554202 knockdown. E, Immunohistochemistry of EZH2 in tumor tissue and normal tissue. F, The expression of miR-31 mRNA was measured in chordoma cells following LOC554202 knockdown with or without 3-deazaneplanocin A treatment; $**P < .01$ versus pcDNA3.0 or control, Student's *t* test

overexpression of LOC554202, but could be restored by the EZH2 inhibitor, 3-deazaneplanocin A (Figure 4F). These data suggested that LOC554202 was negatively correlated with miR-31 expression by recruiting EZH2.

3.5 | RNF144B was a target of miR-31

TargetScan 6.2 and miRanda were used to predict the target of miR-31. As shown in Figure 5A, RNF144B was found to be a novel oncogene

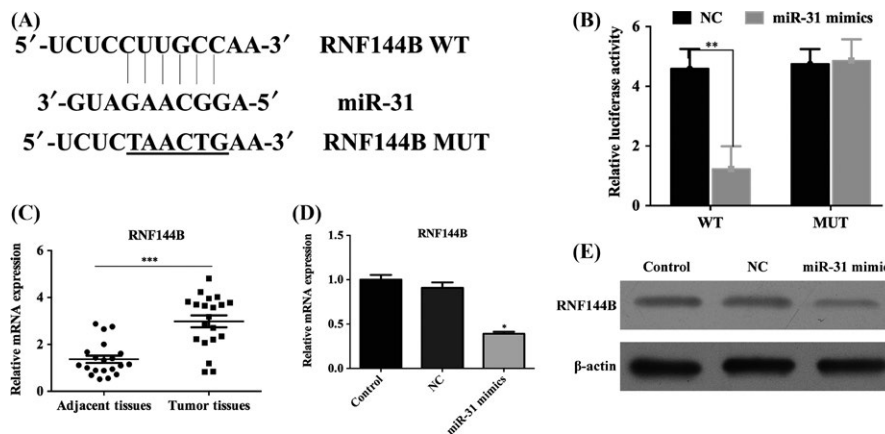


FIGURE 5 RNF144B was a direct target of miR-31 in chordoma. A, Bioinformatic analysis identified a potential miR-31 target site in the 3'-UTR of RNF144B. B, 293T cells were cotransfected with wild-type or mutated RNF144B 3'-UTR reporter constructs and miR-31 mimics or negative control. Firefly luciferase activity was normalized to Renilla luciferase activity. $**P < .01$ versus NC, Student's *t* test. C, The mRNA level of RNF144B was determined in chordoma tissues and normal tissues using qRT-PCR analysis. $***P < .001$ versus normal tissues, Student's *t* test. D and E, The mRNA and protein expression of RNF144B were measured in U-CH1 cells transfected with miR-31 mimics or NC. $*P < .05$, Student's *t* test

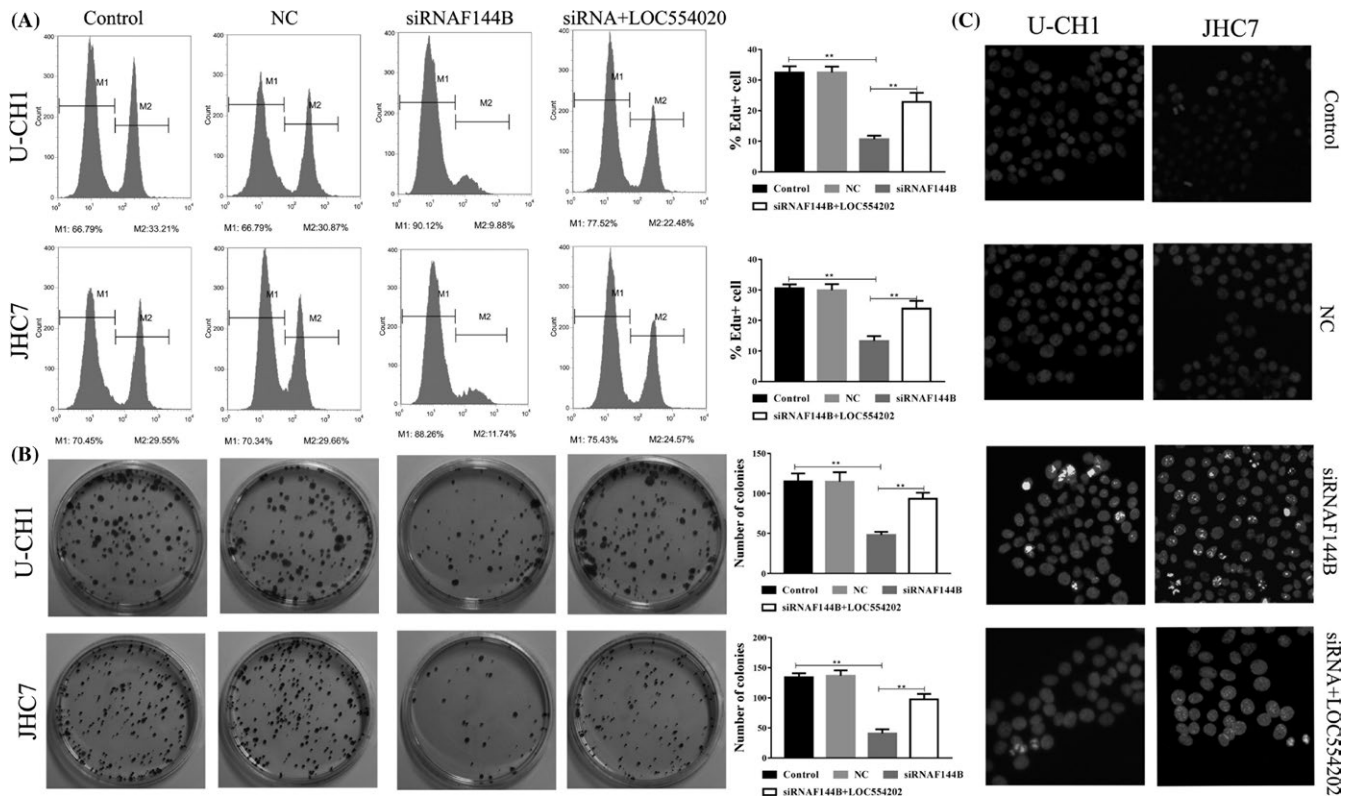


FIGURE 6 Downregulation of RNF144B inhibited cell proliferation and promoted apoptosis in chordoma. A, EdU flow cytometry was used to investigate the percentage of EdU positive cells in U-CH1 and JHC7 cells after transfection with siRNF144B. B, Colony formation analysis of cell proliferation in U-CH1 and JHC7 cells after transfection with siRNF144B, pcDNA 3.0-LOC554202 or NC. C, Hoechst staining assay was used to analyze the percentage of cells with fragmented nuclei in U-CH1 and JHC7 cells after transfection with siRNF144B or NC. ** $P < .01$

targeted by miR-31. To examine whether miR-31 directly binds to the 3'-UTR of RNF144B, we used the Luciferase Reporter Assay after transfecting 293T cells with psiCHECKTM-2-RNF144B-3'-UTR together with miR-31 mimics, mutational miR-31, or NC. The results indicated that luciferase activity was decreased when psiCHECKTM-2-RNF144B-3'-UTR was cotransfected with miR-31 mimics, but was unchanged with mutational miR-31 mimics (Figure 5B, $P < .01$). Furthermore, we found that the expression of RNF144B mRNA was significantly upregulated in chordoma tissues, which suggested it might be a novel oncogene in chordoma (Figure 5C, $P < .001$). In addition, overexpression of miR-31 decreased RNF144B expression, as determined by qRT-PCR (Figure 5D, $P < .01$) and Western blot analysis (Figure 5E). These findings further supported that RNF144B was the target of miR-31.

3.6 | Knockdown of RNF144B suppressed cell proliferation and promoted apoptosis in chordoma

RNF144B has been shown to be overexpressed in chordoma, which is targeted by miR-31. To further investigate its role in chordoma, we performed loss-of-function experiments in U-CH1 and JHC7 cells. As shown in Figure 6A, the positive fluorescence rate was significantly lower in the NC group (30.0%) compared with the siRNF144B group (8.5%) in U-CH1 cells. A similar trend was also observed in JHC7 cells. Moreover, fewer and smaller colonies were found in

U-CH1 and JHC7 cells transfected with siRNF144B compared with NC, or Control groups (Figure 6B). We also investigated whether knockdown of RNF144B affects cell apoptosis as measured by the Hoechst staining assay. As shown in Figure 6C, the number of cells with fragmented nuclei was notably increased in the siRNF144B group compared with the NC or Control groups in both U-CH1 and JHC7 cells. All these RNF144B-induced effects could be restored by overexpression of LOC554202. These results suggested that RNF144B plays a positive role in tumour cell growth in chordoma in vitro.

3.7 | Knockdown of RNF144B inhibited cell migration and invasion by altering EMT expression

We next investigated the effect of RNF144B on chordoma cell migration and invasion. The results of Transwell assays revealed that inhibition of RNF144B decreased U-CH1 and JHC7 cell migration and invasion (Figure 7A). qRT-PCR and Western blot assays demonstrated that siRNF144B treatment increased the expression of the epithelial markers cytokeratin and E-cadherin, and decreased the expression of the mesenchymal markers N-cadherin and vimentin in U-CH1 and JHC7 cells (Figure 7B, C). All these RNF144B-induced effects could be restored by overexpression of LOC554202. Taken together, these results indicated that RNF144B possesses metastasis-promoting activity and may be a novel oncogene in chordoma.

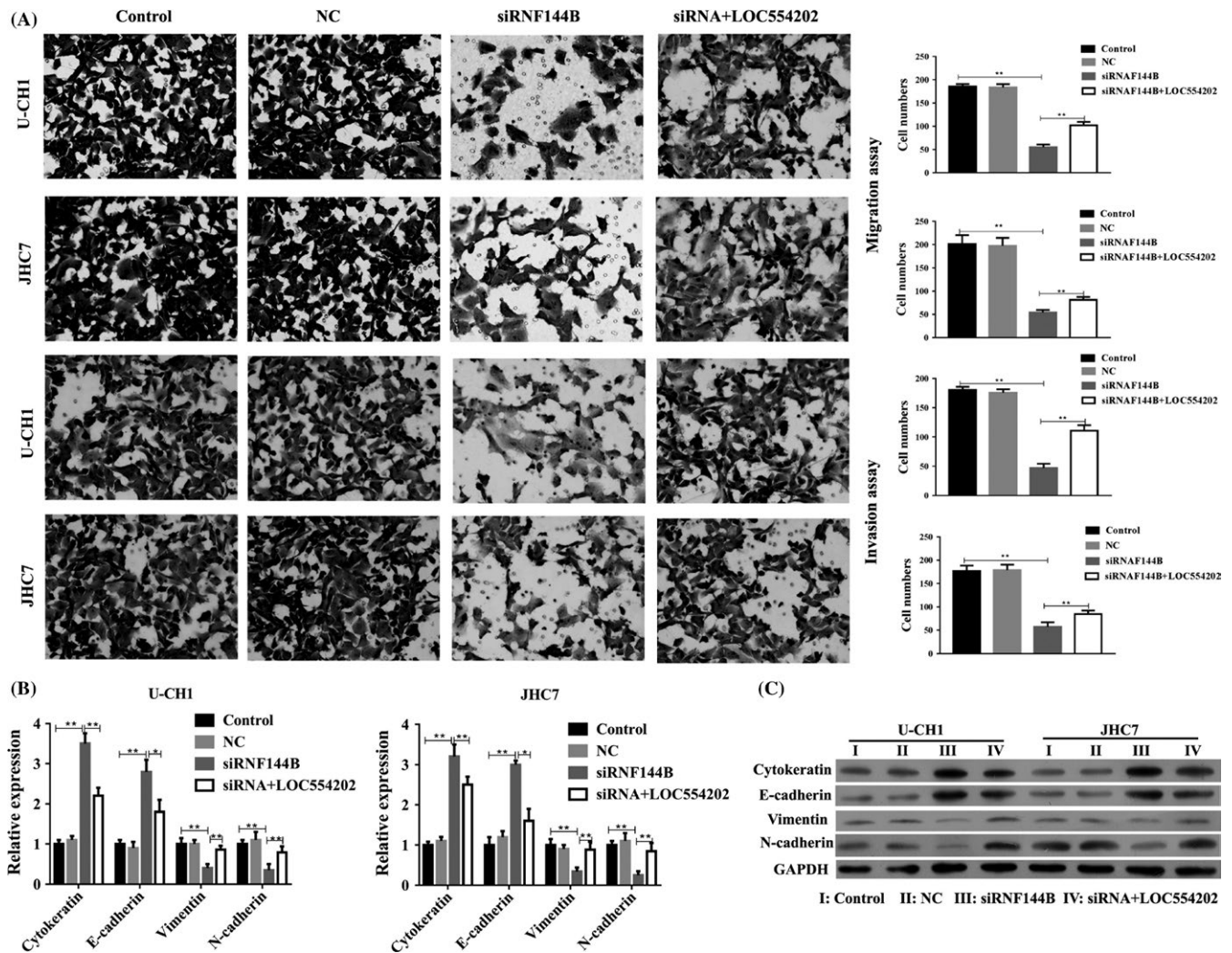


FIGURE 7 Downregulation of RNF144B suppressed chordoma cell migration, invasion, and EMT. A, Transwell assays were used to investigate the changes in migratory and invasive ability of chordoma cell lines, U-CH1 and JHC7. B, qRT-PCR was used to detect cytoke-
 ratin, E-cadherin, N-cadherin, and vimentin expression in U-CH1 and JHC7 cells with siRNF144B, pcDNA 3.0-LOC554202 or NC. * $P < .05$, ** $P < .01$, Student's t test. C, Western blot was used to detect cytoke-
 ratin, E-cadherin, N-cadherin, and vimentin expression in U-CH1 and JHC7 cells with siRNF144B

3.8 | LOC554202/miR-31 affects tumourigenesis of chordoma cells in vivo

To further verify, the level of LOC554202/miR-31 expression on tumourigenesis, U-CH1 and JHC7 cells stably expressing siLOC554202, miR-31 mimics, or empty vector were subcutaneously injected into NOD/SCID mice. As shown in Figures 8A, B, the tumours formed in siLOC554202 or miR-31 mimics group were dramatically smaller than those in the empty vector or control groups. In addition, there was a significant decrease in tumour volume in the siLOC554202 and miR-31 mimics groups compared with controls (Figure 8C, D, $P < .05$, $P < .01$). We also determined the expression of EZH2, miR-31, and RNF144B in tumour tissues after knockdown of LOC554202 in tumour-bearing mice. The results confirmed that knockdown of LOC554202 could decrease the EZH2 level to restore the expression of miR-31, which accompanied by the inhibition of EMT phenotype, leading to inhibition of the function of oncogene RNF144B (Figure 8E). These

results suggest that LOC554202/miR-31 expression is significantly associated with the in vivo proliferation capacity of chordoma cells.

4 | DISCUSSION

Dysregulated expression of lncRNAs and miRs is frequently observed in various cancers, where they act as tumour suppressors or oncogenes. A previous study demonstrated that LOC554202, which is the host gene of miR-31, regulates breast cancer cell proliferation and migration.¹⁹ At present, however, the molecular basis of the interaction between LOC554202 and miR-31 in chordoma is still unclear. Here, we aimed to investigate the involvement of LOC554202 and miR-31 and their biological functions in chordoma.

Our data showed that LOC554202 was significantly upregulated in chordoma tissues compared with normal tissues, accompanied by a concomitant decrease in miR-31 expression. We also observed that

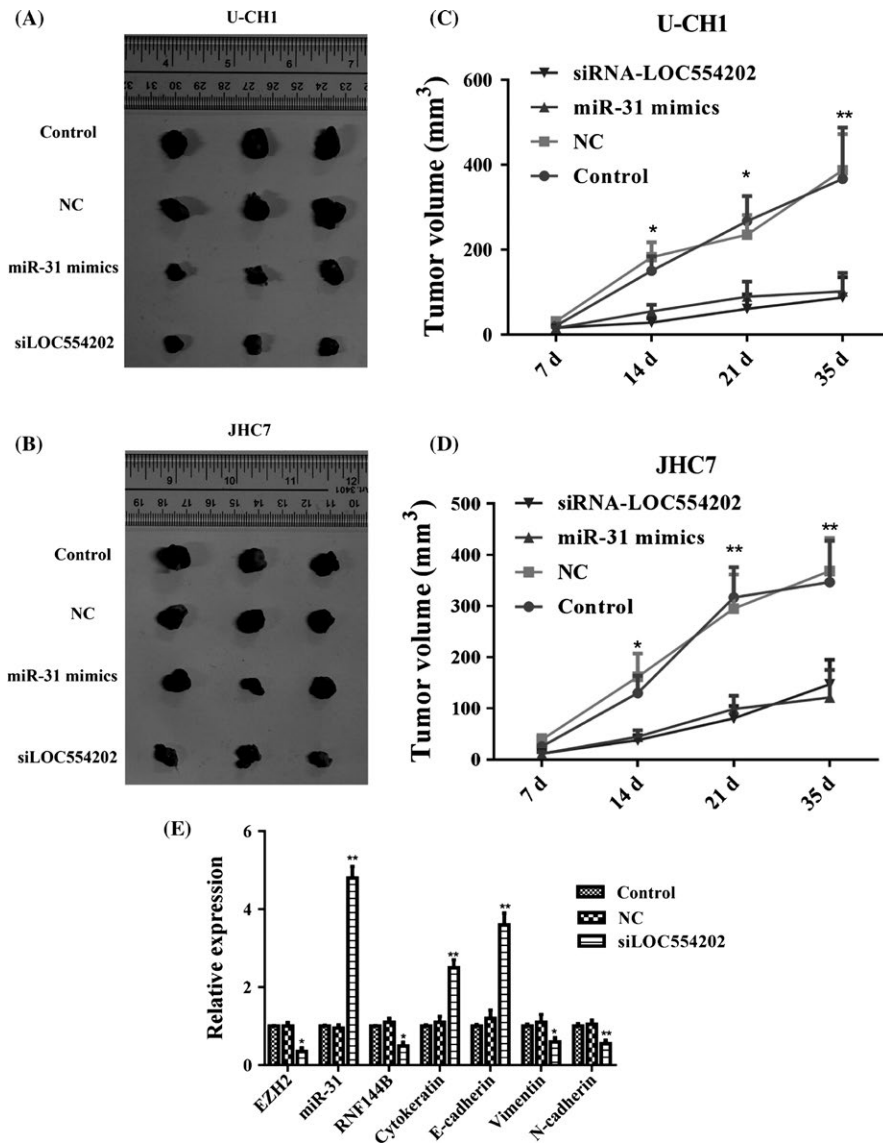


FIGURE 8 The effects of LOC554202 and miR-31 on tumour growth in a xenograft mouse model. A and C, The total visible tumours formed in siLOC554202, miR-31 mimics, NC or control groups, respectively. B and D, The tumour volumes were calculated every 7 days after inoculation. E, After knockdown of LOC554202, the expression of EZH2, miR-31, RNF144B, and EMT markers were estimated in tumour tissues. * $P < .05$, ** $P < .01$ versus NC or control, Student's *t* test

downregulation of LOC554202 suppressed cell proliferation, impaired colony formation ability, promoted cell apoptosis in vitro. Furthermore, siRNA-mediated knockdown of LOC554202 decreased cell migration and invasion by chordoma cells through suppression of EMT expression, as revealed by elevated expression of E-cadherin and reduced expression of N-cadherin and vimentin. These findings were consistent with previous reports showing that LOC554202 promotes tumourigenesis in breast cancer¹⁹ and lung cancer.²⁷ In addition, we also determined the function of miR-31 by performing gain-of-function experiments on chordoma cells. Similar to loss-of-function of LOC554202, overexpression of miR-31 inhibited cell proliferation, migration, and invasion, increased apoptosis in vitro, and suppressed tumour growth in vivo in chordoma; these findings were in agreement with the study of Bayrak and colleagues.²² These results suggested that LOC554202 has oncogenic role, while miR-31 has tumour suppressive role in chordoma.

Although miR-31 is transcribed from the first intron of LOC554202 on human chromosome 9,²⁰ LOC554202 expression was negatively correlated with miR-31 expression in chordoma. We thus guessed

that LOC554202 may have direct effects on its target genes, or act indirectly through specific LOC554202-interacting proteins. Further exploration identified EZH2 as the target gene of LOC554202 using RNA pull down and RIP assay, and RNF144B was identified as the target of miR-31 by the luciferase reporter assay. EZH2, a polycomb protein, has been found to be a tumour promoter frequently involved in variety of human cancers such as prostate cancer and breast cancer.^{28,29} Consistent with previous studies, the expression of EZH2 was significantly upregulated under the condition of LOC554202 overexpression. RNF144B, an E3 ubiquitination ligase, has been shown to be necessary for inflammasome responses in primary human macrophages.³⁰ Although the downstream regulation of RNF144B by miR-31 is not completely understood, we showed that RNF144B was remarkably upregulated in chordoma tissues and that its downregulation reduced cell proliferation, migration, and invasion, and promoted cell apoptosis in chordoma cells. These findings indicated that LOC554202 and miR-31 have different targets and play different roles in different pathways in chordoma progression.

In summary, this study examined the expression of LOC554202 and miR-31 and their biological function in chordoma. Furthermore, we concluded there might be a novel LOC554202/EZH2/miR-31/RNF144B signalling cascade in chordoma. But the complexities of LOC554202 function may be beyond we imagined, and further analysis is needed.

ACKNOWLEDGEMENT

We thank Prof. Gary Gallia (Johns Hopkins University) and the Chordoma Foundation for providing helpful instructions in the overall project.

CONFLICTS OF INTEREST

No competing financial interests exist.

ORCID

Xuwei Xia  <http://orcid.org/0000-0002-6447-8906>

REFERENCES

- Almefty K, Pravdenkova S, Colli BO, Al-Mefty O, Gokden M. Chordoma and chondrosarcoma: similar, but quite different, skull base tumors. *Cancer*. 2007;110:2457-2467.
- Gulluoglu S, Turksay O, Kuskucu A, Ture U, Bayrak OF. The molecular aspects of chordoma. *Neurosurg Rev*. 2016;39:185-196; discussion 196.
- Patel P, Brooks C, Seneviratne A, Hess DA, Seguin CA. Investigating microenvironmental regulation of human chordoma cell behaviour. *PLoS ONE*. 2014;9:e115909.
- Wang L, Zehir A, Nafa K, et al. Genomic aberrations frequently alter chromatin regulatory genes in chordoma. *Genes Chromosomes Cancer*. 2016;55:591-600.
- Gagliardi F, Boari N, Riva P, Mortini P. Current therapeutic options and novel molecular markers in skull base chordomas. *Neurosurg Rev*. 2012;35:1-13; discussion 13-14.
- Chugh R, Tawbi H, Lucas DR, Biermann JS, Schuetze SM, Baker LH. Chordoma: the nonsarcoma primary bone tumor. *Oncologist*. 2007;12:1344-1350.
- Yakkioui Y, van Overbeeke JJ, Santegoeds R, van Engeland M, Temel Y. Chordoma: the entity. *Biochem Biophys Acta*. 2014;1846:655-669.
- Mattick JS, Makunin IV. Non-coding RNA. *Hum Mol Genet*. 2006;15(Suppl. 1):R17-R29.
- Szymanski M, Barciszewska MZ, Erdmann VA, Barciszewski J. A new frontier for molecular medicine: noncoding RNAs. *Biochem Biophys Acta*. 2005;1756:65-75.
- Roberts TC, Morris KV, Wood MJ. The role of long non-coding RNAs in neurodevelopment, brain function and neurological disease. *Philos Trans R Soc Lond B Biol Sci*. 2014;369:1652-1664.
- Tsai MC, Spitale RC, Chang HY. Long intergenic noncoding RNAs: new links in cancer progression. *Can Res*. 2011;71:3-7.
- Bhan A, Mandal SS. Long noncoding RNAs: emerging stars in gene regulation, epigenetics and human disease. *ChemMedChem*. 2014;9:1932-1956.
- Yu SL, Chen HY, Chang GC, et al. MicroRNA signature predicts survival and relapse in lung cancer. *Cancer Cell*. 2008;13:48-57.
- Ozen M, Creighton CJ, Ozdemir M, Ittmann M. Widespread deregulation of microRNA expression in human prostate cancer. *Oncogene*. 2008;27:1788-1793.
- Duan Z, Choy E, Nielsen GP, et al. Differential expression of microRNA (miRNA) in chordoma reveals a role for miRNA-1 in Met expression. *J Orthop Res*. 2010;28:746-752.
- Gao Y, Wu F, Zhou J, et al. The H19/let-7 double-negative feedback loop contributes to glucose metabolism in muscle cells. *Nucleic Acids Res*. 2014;42:13799-13811.
- Yu F, Lu Z, Chen B, Dong P, Zheng J. Identification of a novel lincRNA-p21-miR-181b-PTEN signaling cascade in liver fibrosis. *Mediators Inflamm*. 2016;2016:9856538.
- Ding J, Lu B, Wang J, et al. Long non-coding RNA Loc554202 induces apoptosis in colorectal cancer cells via the caspase cleavage cascades. *J Exp Clin Cancer Res*. 2015;34:100.
- Shi Y, Lu J, Zhou J, et al. Long non-coding RNA Loc554202 regulates proliferation and migration in breast cancer cells. *Biochem Biophys Res Comm*. 2014;446:448-453.
- Corcoran DL, Pandit KV, Gordon B, Bhattacharjee A, Kaminski N, Benos PV. Features of mammalian microRNA promoters emerge from polymerase II chromatin immunoprecipitation data. *PLoS ONE*. 2009;4:e5279.
- Augoff K, McCue B, Plow EF, Sossey-Alaoui K. miR-31 and its host gene lncRNA LOC554202 are regulated by promoter hypermethylation in triple-negative breast cancer. *Mol Cancer*. 2012;11:5.
- Bayrak OF, Gulluoglu S, Aydemir E, et al. MicroRNA expression profiling reveals the potential function of microRNA-31 in chordomas. *J Neurooncol*. 2013;115:143-151.
- Li H, Yu B, Li J, et al. Overexpression of lncRNA H19 enhances carcinogenesis and metastasis of gastric cancer. *Oncotarget*. 2014;5:2318-2329.
- Xu M, Wang Y, Chen L, et al. Down-regulation of ribosomal protein S15A mRNA with a short hairpin RNA inhibits human hepatic cancer cell growth in vitro. *Gene*. 2014;536:84-89.
- Chase A, Cross NC. Aberrations of EZH2 in cancer. *Clin Cancer Res*. 2011;17:2613-2618.
- Benetatos L, Voulgaris E, Vartholomatos G, Hatzimichael E. Non-coding RNAs and EZH2 interactions in cancer: long and short tales from the transcriptome. *Int J Cancer*. 2013;133:267-274.
- Xi S, Yang M, Tao Y, Xu H, Shan J, Inchauste S, Zhang M, Mercedes L, Hong JA, Rao M, Schrupp DS. Cigarette smoke induces C/EBP-beta-mediated activation of miR-31 in normal human respiratory epithelia and lung cancer cells. *PLoS one*. 2010;5:e13764.
- Simon JA, Lange CA. Roles of the EZH2 histone methyltransferase in cancer epigenetics. *Mutation Research/fundamental & Molecular Mechanisms of Mutagenesis*. 2008;647:21-29.
- Bachmann IM, Halvorsen OJ, Collett K, Stefansson IM, Straume O, Haukaas SA, Salvesen HB, Otte AP, Akslen LA. EZH2 expression is associated with high proliferation rate and aggressive tumor subgroups in cutaneous melanoma and cancers of the endometrium, prostate, and breast. *Journal of Clinical Oncology*. 2006;24(2):268-273.
- Ariffin JK, Kapetanovic R, Schaale K, Gatica-Andrades M, Blumenthal A, Schroder K, Sweet MJ. The E3 ubiquitin ligase RNF144B is LPS-inducible in human, but not mouse, macrophages and promotes inducible IL-1 β expression. *Journal of Leukocyte Biology*. 2016.

How to cite this article: Ma X, Qi S, Duan Z, et al. Long non-coding RNA LOC554202 modulates chordoma cell proliferation and invasion by recruiting EZH2 and regulating miR-31 expression. *Cell Prolif*. 2017;50:e12388. <https://doi.org/10.1111/cpr.12388>